Molecular Geometry Fluctuation Model for the Mobility of Conjugated Polymers

Z. G. Yu, D. L. Smith, A. Saxena, R. L. Martin, and A. R. Bishop
Los Alamos National Laboratory, Los Alamos, New Mexico 87545
(Received 11 August 1999)

We present a model to describe electrical transport in dense films of conjugated polymers. The essential physical features of the model are as follows: (i) thermal fluctuations in the molecular geometry of the polymer modify the energy levels of localized electronic states in the material, and (ii) the primary restoring force for these fluctuations is steric, which leads to spatial correlation in the energies of the localized electronic states. The model describes the electric field dependence of the mobility and explains the carrier density dependences of mobility observed in polymer diodes and field effect transistors.

PACS numbers: 72.10.−d, 71.38.+i, 72.80.Le

Electronic devices based on conjugated polymers have attracted much attention [1,2]. Understanding the carrier transport properties in these materials is important in order to design new materials and device structures. Time-of-flight (TOF) measurements show that the electric field (E) dependence of the mobility in many conjugated polymers has approximately the Poole-Frenkel form, i.e., the mobility increases approximately exponentially with $\sqrt{E}$ [3–5]. Bässler and co-workers extensively studied mobility in these materials using Monte Carlo simulations of the Gaussian disorder model (GDM) [6]. The GDM explains some features of the observed mobility; however, as pointed out by Gartstein and Conwell [7], a spatially correlated potential for the carriers is needed to describe the observed Poole-Frenkel behavior. Poole-Frenkel behavior was first observed in molecularly doped polymers, in which the dopant molecules have permanent dipole moments [8,9]. Dunlap and co-workers recently proposed a model for the mobility of molecularly doped polymers based on the long-range interaction between the charged carriers and the dipole moments of the molecular dopants [10]. An essential ingredient of this model is the long-range correlation of carrier energies at different spatial positions that results from the long-range charge-dipole interaction. However, the mechanism leading to the Poole-Frenkel behavior in conjugated polymers cannot be due to charge-dipole interactions, as it is in molecularly doped materials, because most conjugated polymers do not have permanent dipole moments. An alternative mechanism is needed to explain the field dependence of the mobility in conjugated polymers.

There are systematic differences in the mobility parameters of various conjugated polymers that provide a clue to the mechanism leading to the field dependence. Specifically, TOF measurements for holes in poly [2-methoxy,5-(2′-ethyl-hexyloxy)-1,4-phenylene vinylene] (MEH-PPV) and poly(9,9-dioctylfluorene) (PFO) have recently been published [3,11]. The mobility in PFO is about two orders higher than that for MEH-PPV, and the field dependence is much weaker; that is, the coefficient of $\sqrt{E}$ in the exponential is much smaller for PFO than for MEH-PPV. In conjugated polymers such as PPV and its derivatives, the orientation of the phenylene rings can easily fluctuate. In PFO, however, this ring-torsion motion is suppressed by chemical bonding between the phenylene rings. This difference suggests that fluctuations in molecular geometry, specifically in the ring torsion, determines the mobility in these materials.

The restoring force for ring-torsion fluctuations can be intermolecular or intramolecular. The intermolecular restoring force dominates in dense films, because the molecules are closely packed [12]. Fluctuations of the adjacent molecular orientations give rise to a large steric energy. By contrast, the intramolecular restoring force is small: the characteristic energy for the ring-torsion mode of an isolated PPV molecule is quite small [13].

To understand the energetics of fluctuations in molecular geometry in conjugated polymers, as a generic prototype, we carried out AM1 [14] calculations of the total energy of a biphenyl molecule as a function of the twist angle between the two rings [15]. For neutral biphenyl, as shown in the inset of Fig. 1, the energy is almost independent of the torsion angle. However, when we add an extra electron or hole to this system, the total energy of the charged state depends strongly on the torsion angle [16]. Thus there is a strong coupling between the local electronic excitation (carrier) and the relative ring orientation. We also carried out AM1 calculations for a system consisting of three parallel benzene rings with a given separation [15]. We calculated the total energy of the system while rotating the central benzene molecule to estimate the intermolecular restoring force. The results of the calculation show that the intermolecular restoring is dominant over the intramolecular one in densely packed materials.

To describe the role of fluctuations in molecular geometry, we propose a general model for the mobility in dense films of conjugated polymers based on the following Hamiltonian:

$$H = \sum_i \varepsilon_i C_i^\dagger C_i + \frac{K}{2}\int d^3r(\nabla\phi)^2 + \nu\sum_i C_i^\dagger C_i \phi(\mathbf{r}_i) + \frac{s}{2}\int d^3r\,\phi^2(\mathbf{r}) + \sum_{i,j}\eta_{i,j}(C_i^\dagger C_j + \text{H.c.}). \quad (1)$$

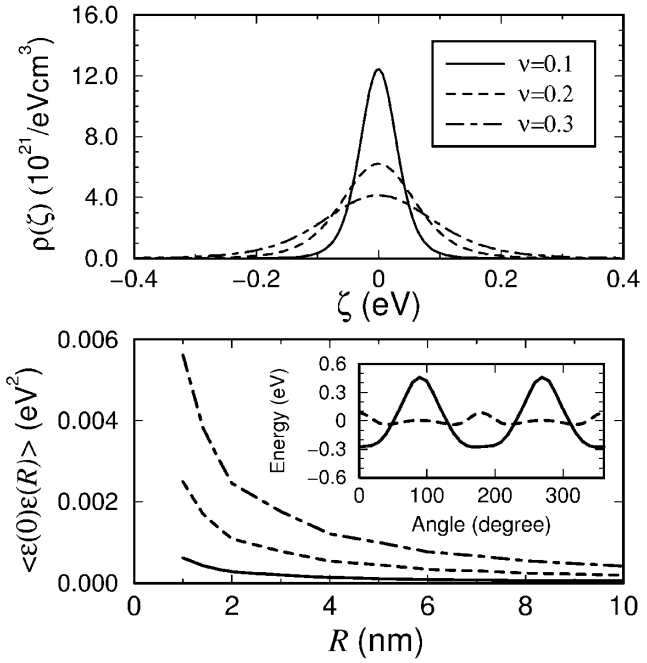

FIG. 1. Distribution (upper panel) and spatial correlation (lower panel) of carrier energies with different polaron-torsion couplings. Solid, dashed, and dot-dashed lines correspond to $\nu = 0.1$, 0.2, and 0.3 eV, respectively. The inset in the lower panel illustrates AM1 results for the total energy as a function of the torsion angle in biphenyl. Dashed and solid lines are for neutral and anion biphenyl, respectively.

Here $C_i^\dagger$ is the creation operator of a carrier (polaron) localized on a site i and ε_i is its bare energy. $\phi(\mathbf{r})$ is the molecular geometry field (in PPV and related materials, it can be regarded as the deviation in torsion angle of the benzene ring) at position $\mathbf{r}$. K is the intermolecular restoring force constant. The gradient of $\phi(\mathbf{r})$ appears in the intermolecular elastic energy because this energy depends on the difference between the torsion angles of adjacent molecules. s is the intramolecular restoring force constant, which is of secondary importance compared to K. As shown in the inset of Fig. 1, the energy minimum in the neutral system occurs at a different angle than in the charged system. Therefore, expanding the energy of the charged system around the equilibrium geometry for the neutral system gives a linear coupling between the polaron and the torsion angle. ν is the coefficient of this linear coupling term. $\eta_{i,j}$ describes polaron hopping between sites. The effect of fluctations in the bare site energies ε_i has been studied in the GDM [6]. Here we consider cases in which energy fluctuations are dominated by the interaction with the molecular geometry field and take the bare site energies all equal to zero.

Because of the coupling between the polaron and the molecular geometry, the polaron energy is a function of position: $\varepsilon(\mathbf{r}_i) = \nu\phi(\mathbf{r}_i)$. By Fourier transforming $\Phi(\mathbf{q}) = \int d^3r\, \phi(\mathbf{r}) e^{i\mathbf{q}\cdot\mathbf{r}}$, the total free energy from the molecular geometry fluctuations is $\Omega^{-1}\sum_{\mathbf{q}} |\Phi(\mathbf{q})|^2 (K\mathbf{q}^2 + s)/2$, where Ω is the volume of the system. The distribution function for the molecular geometry fluctuations is

$$D(\{\Phi(\mathbf{q})\}) \propto \exp\left[-\frac{\Omega^{-1}\sum_{\mathbf{q}} |\Phi(\mathbf{q})|^2 (K\mathbf{q}^2 + s)/2}{k_B T} \right], \quad (2)$$

where T is the temperature and k_B is the Boltzmann constant. Equipartition of energy gives

$$\left\langle \Omega^{-1} |\Phi(\mathbf{q})|^2 \left(\frac{K}{2}\mathbf{q}^2 + \frac{s}{2} \right) \right\rangle = \frac{1}{2} k_B T . \quad (3)$$

Thus we obtain the spatial correlation of polaron energies,

$$\langle \varepsilon(\mathbf{r}_1)\varepsilon(\mathbf{r}_2)\rangle = \nu^2 \langle \phi(\mathbf{r}_1)\phi(\mathbf{r}_2)\rangle = \frac{\nu^2 k_B T}{4\pi K R} e^{-\alpha R}, \quad (4)$$

where $R = |\mathbf{r}_1 - \mathbf{r}_2|$ and $\alpha = \sqrt{s/K}$. Equation (2) describes the distribution function for fluctuations without including the interaction with the carrier. The effects of this coupling can be included by taking the expectation value of the Hamiltonian with the carrier at a specific molecular site and completing the square to eliminate the linear term in ϕ. This treatment again gives a Gaussian distribution function with a modified field variable. It does not change the results presented here [15].

For one-dimensional (1D) systems, the field-dependent mobility has been exactly obtained [17], and, in a continuum limit, it can be written as [10,18]

$$\mu = \frac{\mu_0}{\gamma \int_0^\infty dy\, e^{-\gamma y} \langle e^{-\beta\varepsilon(0)+\beta\varepsilon(y)}\rangle}, \quad (5)$$

where $\gamma = \beta e E$, e is the electron charge, and $\beta = (k_B T)^{-1}$. Substituting the correlation function in the small s limit into Eq. (5) gives

$$\mu = \frac{\mu_0 e^{-\beta\sigma^2}}{\beta\sqrt{2\pi\sigma^2 a e E}\, K_1(\beta\sqrt{2\pi\sigma^2 a e E})}, \quad (6)$$

where $\sigma^2 = \nu^2/(2\pi^2 K a)$, $1/a$ is a momentum cutoff, and $K_1(z)$ is the first-order modified Bessel function of the third kind. Using the asymptotic expansion for $K_1(z)$, the mobility is $\mu \sim e^{-\beta\sigma^2} e^{\beta\sqrt{E}\sqrt{2\pi\sigma^2 a e}}$. Our model and the charge-dipole model give the same field dependence of mobility, $\ln\mu \sim \sqrt{E}$, but they give a different temperature dependence: $\ln\mu \sim \beta$ here compared to $\ln\mu \sim \beta^2$ in the charge-dipole model.

We do not expect the 1D result to be valid for dense three-dimensional (3D) films. In 3D systems, the carrier can take an optimal path to avoid high energy barriers [15]. We study the mobility in a 3D lattice by solving the steady state master equation for the system:

$$0 = \sum_j [\omega_{ij} P_j (1 - P_i) - \omega_{ji} P_i (1 - P_j)]. \quad (7)$$

Here P_i is the probability for the polaron to be on site i and ω_{ij} is the polaron hopping rate from site j to site

i. We have excluded double occupation at a site. After finding the solution P_i to Eq. (7), we calculate the velocity from $\mathbf{v} = \sum_{ij} \omega_{ji} P_i (1 - P_j) \mathbf{R}_{ji}$, $\mathbf{R}_{ji} = \mathbf{r}_j - \mathbf{r}_i$, and the mobility from $\mathbf{v} = \mu \mathbf{E}$. Compared with Monte Carlo simulations, the master equation approach has several advantages: it guarantees the steady state solution; it is more convenient for considering density-dependent effects; and it is numerically more efficient.

We generate the molecular geometry fluctuations and, accordingly, polaron energies on each site. Then we solve the master equations using a symmetric hopping rate in the presence of an applied electric field $\mathbf{E}$,

$$\omega_{ji} = \omega_0 e^{-2\Gamma(R_{ij}/a)} e^{(\beta/2)[\varepsilon(\mathbf{r}_i) - \varepsilon(\mathbf{r}_j) - e\mathbf{E}\cdot\mathbf{R}_{ji}]}. \quad (8)$$

We include first and second nearest neighbor hopping. The system size is $64 \times 32 \times 32$, the lattice constant is $a = 10$ Å, $2\Gamma = 10$, and the applied field is along the x axis. We use the distribution function, Eq. (2), to generate the spatially correlated molecular geometry fluctuations. There is no correlation among the molecular geometry fluctuations in momentum space $\Phi(\mathbf{q})$ for different $\mathbf{q}$. We generate distributions of $\Phi(\mathbf{q})$ and then Fourier transform to get $\phi(\mathbf{r})$, which have the correlation given by Eq. (4).

Figure 1 shows the polaron energy distribution and the spatial correlation between polaron energies with different polaron-torsion coupling ν for a fixed intermolecular force constant $K = 0.0034$ eV/Å. This value for K was chosen to match with measured mobilities for MEH-PPV; it is consistent with the calculated estimate for this restoring force described above. Here s is set to zero and the temperature is $T = 300$ K. The energy distribution is calculated by $\rho(\zeta) = \frac{1}{\Omega} \sum_i \delta[\varepsilon(\mathbf{r}_i) - \zeta]$. The polaron energy in the system has a Gaussian distribution with width depending on coupling ν [15].

We consider the field-dependent mobility in the dilute limit by linearizing the master equation. We present the field-dependent mobility in Fig. 2 using the same parameters as in Fig. 1. The curves are reasonably close to linear, showing that the model gives approximately the Poole-Frenkel form. For a more dispersive system (e.g., $\nu = 0.3$), the mobility is low and has a strong field dependence; whereas, for a more ordered system (e.g., $\nu = 0.1$), the mobility is higher and has a weaker field dependence.

The mobility depends on carrier density because, when some carriers fill deep potential sites, the others become more mobile. The density dependence of mobility is studied by solving the nonlinear master equation. We have developed an iteration approach to solve these nonlinear equations [15]. In Fig. 3, we illustrate the carrier density effects on the mobility. We see that the mobility is enhanced by almost 1 order of magnitude with increase of the carrier density to $n = 6.9 \times 10^{18}$ cm^{-3} at $E \sim 4 \times 10^4$ V/cm. In the low-field regime, where the field-assisted jumping for carriers is less efficient than in the high-field regime, the carrier density effect on mobility is more pronounced.

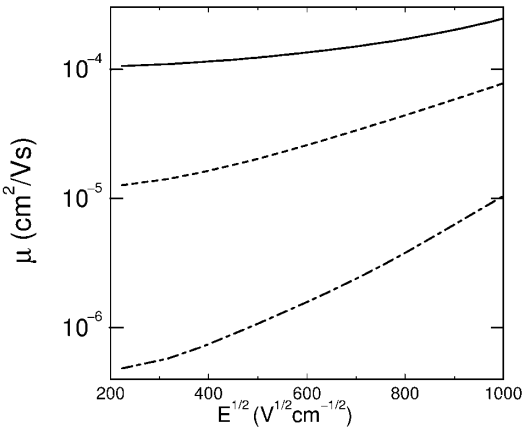

FIG. 2. Logarithm of mobility μ against $E^{1/2}$ with different polaron-torsion couplings. Solid, dashed, and dot-dashed lines correspond to $\nu = 0.1$, 0.2, and 0.3 eV, respectively. Other parameters are the same as in Fig. 1.

TOF experiments are low carrier density measurements. Carrier mobility in conducting polymers is also investigated in electrical device measurements using polymer diode and field-effect transistor current-voltage characteristics. Because of the different structure of these devices, they sample very different field and carrier density regimes. Experiments in polymer diodes sample relatively high electric fields and low carrier densities, whereas experiments in field-effect transistors sample relatively high carrier densities and low fields. Recent diode measurements show that, at electric fields of a few times 10^6 V/cm, there is not a strong carrier density dependence of the mobility in MEH-PPV for densities up to about 10^{18} cm^{-3} [19]. Field-effect transistor measurements have suggested

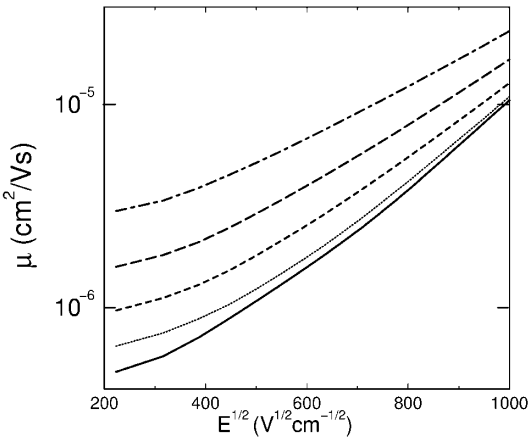

FIG. 3. Logarithm of mobility μ against $E^{1/2}$ with different carrier densities for $\nu = 0.3$ eV, $K = 0.0034$ eV/Å, and $T = 300$ K. Dotted, short-dashed, long-dashed, and dot-dashed lines correspond to carrier density $n = 0.08$, 0.5, 2, and 6.9×10^{18} cm^{-3}, respectively. The solid line shows the result of solving the linearized master equations.

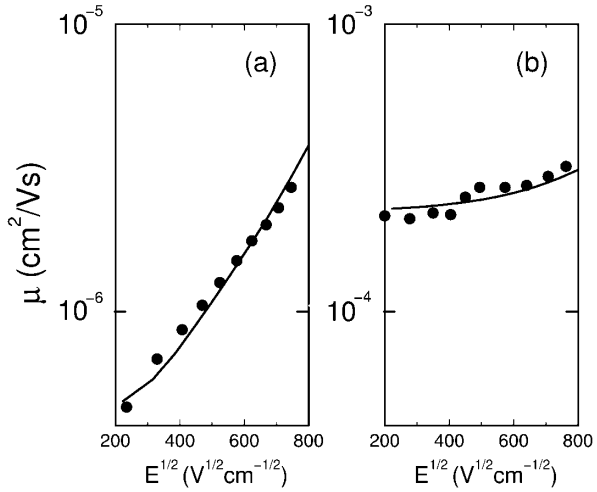

FIG. 4. Field-dependent mobility plotted on logarithm vs $E^{1/2}$ scale. In panel (a), dots are experimental data for MEH-PPV (Ref. [3]), and the solid line is our theoretical result with $\nu = 0.3$ eV, $K = 0.0034$ eV/Å, and $T = 300$ K. In panel (b), dots are experimental data for PFO (Ref. [11]), and the solid line is our theoretical results with $\nu = 0.3$ eV, $K = 0.01$ eV/Å, and $T = 300$ K.

that the mobility increases strongly with increasing carrier density at low fields (typically below a few 10^4 V/cm) for carrier densities above about 10^{18} cm^{-3} [20]. Our calculated results are consistent with both of these types of device measurements and show why this qualitatively different behavior is expected when the different field/density regimes are sampled.

To interpret TOF mobility measurements in MEH-PPV and PFO [3,11], we fit the mobility data of MEH-PPV [3] by adjusting the parameters ν and K around the values estimated from the AM1 calculations for biphenyl and the three-benzene system: $\nu \sim 0.4$ eV per radian and $K \sim 0.002$–0.005 eV/Å. We find a good fit, as shown in Fig. 4(a), can be obtained by using $\nu = 0.3$ eV and $K = 0.0034$ eV/Å. Torsion fluctuations are strongly suppressed by chemical bonding in PFO and we use a larger K to model this situation. Using $\nu = 0.3$ eV and $K = 0.01$ eV/Å, we find that the theoretical results are in good agreement with the experimental data for PFO [11], as shown in Fig. 4(b).

In summary, we have proposed a model to describe electrical transport in dense films of conjugated polymers in which thermal fluctuations in the molecular geometry modify the energy levels of localized (polaronic) electronic states. The primary restoring force for these fluctuations is steric in origin. Because the restoring force is intermolecular, there is a spatial correlation in the molecular distortions which leads to a spatial correlation in the energies of the localized states. The model explains the experimentally observed field and carrier density dependence of the mobility and provides a general framework to understand the transport in conjugated polymers.

We are grateful to I. H. Campbell, E. M. Conwell, D. H. Dunlap, and S. V. Novikov for helpful discussions. This work was supported by the U.S. Department of Energy.

[1] J. H. Burroughes *et al.*, Nature (London) **347**, 539 (1990).
[2] J. R. Sheats *et al.*, Science **273**, 884 (1996).
[3] I. H. Campbell, D. L. Smith, C. J. Neef, and J. P. Ferraris, Appl. Phys. Lett. **74**, 2809 (1999).
[4] P. W. Blom, M. J. M. Dejong, and M. G. VanMunster, Phys. Rev. B **55**, R656 (1997).
[5] M. Abkowitz, H. Bässler, and M. Stolka, Philos. Mag. B **63**, 201 (1991).
[6] H. Bässler, Phys. Status Solidi (b) **175**, 15 (1993).
[7] Yu. N. Gartstein and E. M. Conwell, Chem. Phys. Lett. **245**, 351 (1995).
[8] D. M. Pai, J. Chem. Phys. **52**, 2285 (1970).
[9] W. D. Gill, J. Appl. Phys. **43**, 5033 (1972).
[10] D. H. Dunlap, P. E. Parris, and V. M. Kenkre, Phys. Rev. Lett. **77**, 542 (1996); S. V. Novikov *et al.*, Phys. Rev. Lett. **81**, 4472 (1998).
[11] M. Redecker, D. D. C. Bradley, M. Inbasekaran, and E. P. Woo, Appl. Phys. Lett. **73**, 1565 (1998).
[12] D. Chen, M. J. Winokur, M. A. Masse, and F. E. Karasz, Phys. Rev. B **41**, 6759 (1990).
[13] K. Pichler *et al.*, J. Phys. Condens. Matter **5**, 7155 (1993).
[14] H. J. S. Dewar, E. G. Zoebisch, and E. F. Healy, J. Am. Chem. Soc. **107**, 3902 (1985).
[15] Z. G. Yu, D. L. Smith, A. Saxena, R. L. Martin, and A. R. Bishop (unpublished).
[16] The calculated results for the biphenyl cation are very similar to those for the anion.
[17] B. Derrida, J. Stat. Phys. **31**, 433 (1983).
[18] P. E. Parris, M. Kuś, D. H. Dunlap, and V. M. Kenkre, Phys. Rev. E **56**, 5295 (1997).
[19] I. H. Campbell, D. L. Smith, C. J. Neef, and J. P. Ferraris, Appl. Phys. Lett. **75**, 841 (1999).
[20] See, for example, C. D. Dimitrakopoulos, S. Purushothaman, J. Kymissis, A. Callegare, and J. M. Shaw, Science **283**, 822 (1999).